Sub-TeV Gamma-Ray Astrophysics using Large Air Čerenkov Telescopes

Toru TANIMORI*)

Department of Physics, Graduate School of Science
Kyoto University, Kyoto 606-8502

(Received)

In 1990's Very High Energy Gamma-ray Astrophysics has dramatically advanced due to the advent of Imaging Air Čerenkov Telescopes(IACTs), and has been widely recognized as an important field of astronomy. After the first detection of persistent TeV gamma-ray emission from the Crab in 1989, several type of TeV gamma-ray sources have been detected and established. Successive discoveries of active galactic nuclei emitting TeV gamma rays after 1992 especially astonished and enabled us directly to watch the high energy phenomena around the huge black holes at the center of galaxies. Recent detections of TeV gamma-ray emission from several supernova remnants have been reported in both southern and northern skies, which had been eagerly looked forward since the beginning of cosmic-ray physics. Those are expected to be a clue of not only the galactic cosmic-ray origin but also the understanding of the particle acceleration due to a diffusive shock.

At first we present the recent observational results and the understanding of high energy phenomena in gamma-ray sources, particularly galactic TeV gamma-ray sources. A brief review of experimental aspect of Very High Energy gamma-ray Astronomy are also described including the perspective of TeV gamma-ray astronomy in the next decade.

§1. Introduction

High energy astronomy is a new field of astronomy grew in the latter half of 20th century by the advent of new astronomical probes of high energy photons, namely, X-rays and Gamma rays. Figure 1 shows the increase of the number of known celestial sources during recent 40 years in X-ray, gamma-ray(GeV region), and very high energy gamma-ray(TeV region) astronomy, respectively. As is well known, X-ray astronomy is established as one of the most vital and valuable fields in astronomy, where several hundred thousands of X-rays sources have been found. On the other hands, the growth of gamma-ray sources had been relatively slow until the launch of the advanced gamma-ray satellite, Compton Gamma-Ray Observa-

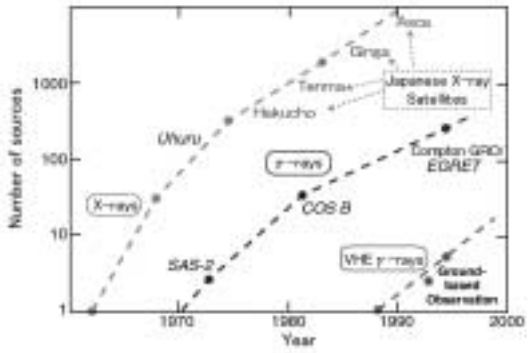

Fig. 1. Increase of the number of known celestial sources during recent 40 years in X-ray, medium energy gamma-ray, and TeV gamma-ray astronomy.

*) A collaborator of the CANGAROO group

tory(CGRO), in 1991 [1]. EGRET, a detector observing GeV gamma rays on-board CGRO, has found more than 200 sources emitting high energy gamma rays during this decade, whereas about 20 sources had been known in this energy region before then. Emissions of high energy gamma rays were observed not only from galactic sources such as pulsar/nebulae, molecular clouds,and supernova remnants but also the more than hundred extragalactic sources. In particular it was very astonishing that almost all extragalactic sources detected, except the Large Magellanic Cloud were coincident to active galactic nuclei located at cosmological distances. Figure 2 shows the GeV gamma-ray source catalog detected by EGRET in galactic coordinates. You can see that hundreds of AGN were located out of the galactic plane, and moreover along the galactic plane there concentrated lots of unidentified sources, which are mainly due to the insufficient angular resolution of EGRET of about 1 degree and intense diffuse galactic gamma rays. In addition, six sources emitting Very high energy gamma rays are drawn in Fig.2.

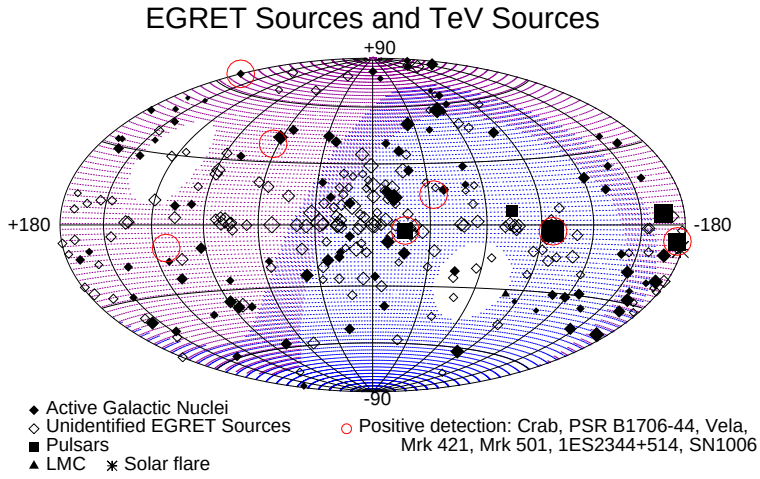

Fig. 2. GeV gamma-ray source catalog detected by EGRET in galactic coordinates, where six TeV gamma-ray sources are also drawn by a circle.

In this decade several TeV gamma-ray sources have been firmly established: Crab pulsar/nebula [2], Mrk421 [3], Mrk501 [4], PSR1706-44 [5]. Celestial objects emitting very high energy gamma rays of energies greater than TeV had been expected as a natural consequence of the existence of Cosmic rays, and they have been searched since the middle of 20th century using the ground based detectors such as scintillation-counter arrays and air Čerenkov telescopes. However, although marginal detections of TeV gamma ray sources were sometimes reported, no persistent TeV gamma-ray source had been found until the discovery of persistent TeV gamma-ray emission from the Crab by the Whipple group in 1989 [2]. Huge background of hadron showers overwhelms the tiny signal of celestial gamma rays of which flux is less than one per thousands of hadron showers. The Whipple group developed the imaging technique proposed by Hillas [6], and hence the rejection power of hadron showers was greatly improved. This technique combined with the large 10m telescope gave

them this great achievement. In 1990's almost all groups searching TeV gamma-ray sources had adopted the imaging technique, and several type of TeV gamma-ray sources have been detected with high statistics. In particular, successive discoveries of Active Galactic Nuclei (AGN) emitting TeV gamma rays after 1992 were astonishing, and enabled us directly to watch the high energy phenomena around huge black holes located at the center of galaxies [3),4)].

Our group, CANGAROO, the collaboration of 14 Japanese institutes and University of Adelaide , has observed TeV gamma-ray sources in the southern hemisphere since 1992 at Woomera in South Australia, using 3.8m telescope with the fine imaging camera [7)]. The southern hemisphere provides us a good chance of the observation for many galactic objects such as pulsar/nebulae, supernova remnants (SNRs), black holes, the galactic center, and so on. In fact we have found several galactic TeV gamma ray sources as listed in Table I in which TeV gamma-ray sources are classified according to their reliabilities by Weekes [8)].

Class	Objects	Observed Group	Specification
Grade A	Crab	Many	Plerion
($> 5\sigma$,	PSR1706-44	CANGAROO, Durham	Plerion
multiple)	Mkn421	Many	AGN(HBL)
	Mkn501	Many	AGN(HBL)
Grade B	SN1006	CANGAROO	SNR
($> 5\sigma$)	Vela	CANGAROO	Plerion
	RXJ1713.7-3946	CANGAROO	SNR
	PKS2155-304	Durham	AGN(HBL)
	1ES1959+650	Utah7TA	AGN(HBL)
	BL Lac	Crimea	AGN(HBL)
Grade C	Cas-A	HEGRA CT	SNR
(strong but	Cen X-3	Durham	X-ray binary
with some	1ES2344+514	Whipple	AGN(HBL)
qualifications)	3C66A	Crimea	AGN
	Geminga	Crimea	Pulsar
	B1509-58	CANGAROO	Plerion

Table I. TeV gamma-ray sources detected by IACTs

Another noteworthy discovery is the several recent reports on the detection of TeV gamma-ray emissions from shell-type SNRs in both southern and northern skies [13),15),16)], which have been eagerly looked forward ever since the beginning of cosmic-ray physics. These detections are expected the direct observation of the site of the particle acceleration by diffusive shocks, and would bring us some answer on the cosmic ray origin in the Galaxy.

Thus several significant advances of high energy gamma-ray astronomy have let us strongly impress another aspect of the universe beyond the well-know thermal universe, which are governed by non-thermal phenomena such as particle acceleration. Here I present good examples of astrophysical high energy phenomena of particle acceleration in celestial objects, and also briefly introduce the imaging Čerenkov technique and Imaging Čerenkov Telescopes (IACTs) for detecting TeV gamma rays. Finally the perspective of TeV gamma-ray astronomy is commented.

§2. Cosmic-ray Origin and Shock Acceleration

High energy particles are known to fill all over the galaxy and maybe to the extended halo, and play non-negligible roles on almost all phenomena in the universe. Furthermore, high energy particles coming to the earth, "Cosmic rays", are surely affected on the circumstance of the earth, i.e., presumably the evolution of a creature. However, nobody know how and where such high energy particles are generated in the universe. These questions are unresolved yet, and always important issues in astrophysics in spite of the long history of the study of cosmic rays.

New astronomical observation probes such as radio and X-ray have revealed lots of high energy phenomena in the universe where huge amount of energy is consumed to accelerate particles up to more than GeV energies. Since high energy electrons emit synchrotron radiation of radio to X-ray in the magnetic field of several micro gauss, observations of synchrotron spectra in theses wavelength have let us know the existence of celestial high energy electrons since 1950s. Also high energy ions (mainly proton) must surely exist in the galaxy since almost all the cosmic rays coming to the earth are ions. The spectrum of cosmic ray observed on the earth extends up to energies 10^{20} eV with power law index of $\sim$ -2.7 [17]

For a long time, supernova remnants (SNRs) have been believed a to be a favored site for accelerating cosmic rays up to 10^{15}eV, because only they can satisfy the required energy input rate to the galaxy among several galactic objects which show high energy phenomena [18]. In addition, a shock acceleration theory was established around 1980s, in which particles are accelerated with the collisions between particles and plasma gas moving at a supersonic velocity in space. This mechanism can accelerate particles more efficiently than the original idea of E.Fermi (2nd order statistical acceleration) by the existence of strong shocks in plasma gas [19), 20]. SNRs are a just extended and heated gas system accompanied by very strong shocks. Furthermore shocks are very common phenomena in the universe, and hence this mechanism has been widely applied for almost all the high energy phenomena in the universe. Nowadays the shock-acceleration mechanism has been a standard theory for particle acceleration in astrophysics. Although this theory looks very simple and reliable, direct observational evidences supporting this are still very sparse. In particular, few observations have been reported on the acceleration of particles up to the relativistic energies. A good review of shock acceleration by Ellison is included in this volume.

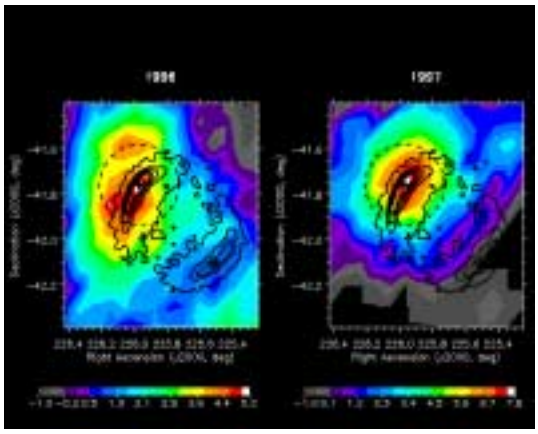

Fig. 3. Map of TeV gamma-ray emission of SN1006 with the contour of X-ray emission by ASCA

In order to investigate the shock-acceleration mechanism, SNR is an unique ideal

laboratory because it is quite simple and a well-understood astronomical object. The evolution of SNR is fairly explained with several observable or well-known parameters such as explosion energy of the SNR, total mass of the ejecta, density of inter stellar medium (ISM) around the SNR and age after the explosion, which are called **Sedov** solution [21]. On the other hand, pulsars or AGN have an active central engine (neutron star or black hole) continuously or intermittently supplying a huge amount of energy for particle acceleration, which makes the numerical understanding very difficult. In addition, the resoluble size of a SNR enables us direct observation of the shock front accelerating particles, which provides lots of significant physical parameters quantitatively (absolute value of the magnetic field, index of power law, maximum energy, diffusion constant, shock velocity, etc.) and its spatial structure (directions of the magnetic field and the shock, distributions of ejecta and ISM). The first reliable evidence for the efficient particle acceleration in a SNR has been presented by the observation of the strong synchrotron emission of SN1006 by the Japanese X-ray satellite ASCA in 1995 [22]. By assuming the conventional galactic magnetic field of a few μ gauss, synchrotron X-ray emission strongly supported the existence of high energy electrons at tens or hundreds TeV. Those high energy electrons emit not only synchrotron radiation but also high energy gamma rays due to Inverse Compton (IC) process by the hard-collision with soft seed photons such as 2.7K Cosmic Microwave Background (CMB). Scattered photons were obtained the energy of about one tenth of primary electrons, and hence reaches near 100 TeV in SN1006 which could be detected by the CANGAROO telescope in the TeV region if the magnetic field were weaker than $\sim 10 \mu$gauss [9) - 12)]. In 1996 and 1997, CANGAROO actually succeeded in detecting the TeV gamma-ray emission from the north rim of SN1006 [13], where the more intense X-ray synchrotron emission was observed as shown in Fig.3.

There exists a simple but useful formula connecting among relativistic electrons, high energy photons scattered by IC process, synchrotron photons and soft seed photons. The emission powers of synchrotron radiation and IC scattering, P_{sync} and P_{IC} are respectively expressed as follows,

$$P_{sync} = \frac{4}{3}\sigma_T c\gamma^2\beta^2 U_B, \quad P_{IC} = \frac{4}{3}\sigma_T c\gamma^2\beta^2 U_{soft}, \qquad (2\cdot1)$$

where σ_T is the Thomson cross section, $\sigma_T = 6.7 \times 10^{-25} cm^2$, and $c\beta$ and γ are the velocity and Lorentz factor of the electron. U_B and U_{soft} are energy densities of the magnetic field and the soft seed photons, respectively.

Since the energy density of soft seed photons, CMB, is well-known and uniform, very high energy gamma-ray observations provide a good estimation of the magnetic field strength at the acceleration site in SN1006 using the above formula. Figure 4 shows the wide band energy spectrum at the north rim of SN1006 from radio to TeV, and also the fitting result based on the shock model [23]. All data are fitted very well, and several significant parameters, magnetic field(B), power index(a), maximum energy (E_{max}) were able to be determined independently: $B = 4.3\mu$ gauss, a = 2.2, and $E_{max} = 60$ TeV. Here we assumed that the detected TeV gamma-ray emission is mainly due to IC process with very high energy electrons considering the tenuous

shell of ($\leq\sim$0.4 cm^{-3}) [14]. In fact the expected spectrum from π° decay generated

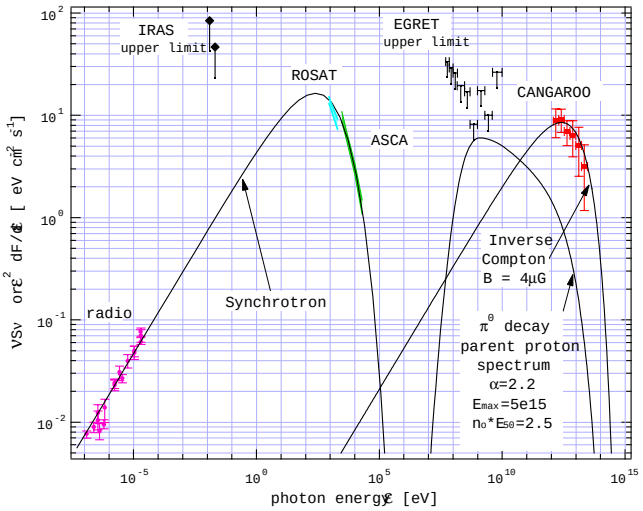

Fig. 4. Energy spectrum at the north rim of SN1006 from radio to TeV, and also fitting results based on the shock model.

by high energy proton conflicts with the upper limit in the GeV region as shown in Fig.4.

In order to verify the origin of cosmic rays, we have to obtain clear evidence of the acceleration of protons. The identification of the parent particles of TeV gamma-rays (electron or proton) will be possible by observing the wide spectrum from Sub to Multi TeV region as shown in Fig.5. Flatter gamma-ray spectrum than -2.0 in this region is surely due to I.C. process, while that due to π° decay generated by collision between ISM and high energy proton is expected to be steeper than -2.0. These study will be soon carried out by the next generation IACTs mentioned later.

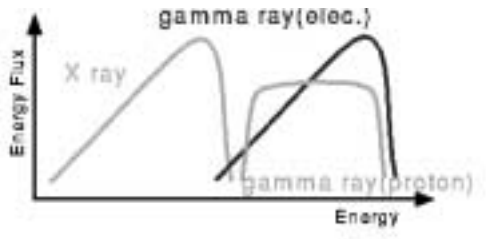

Fig. 5. Expected energy spectra from both IC process and π° decay with synchrotron spectrum.

§3. Galactic Objects emitting TeV Gamma Rays

So far EGRET has found several kinds of celestial objects emitting high energy gamma rays: radio pulsars (pulsed signal), pulsar-nebulae (unpulsed signal), X-ray binary neutron stars, the galactic center, SNRs, molecular clouds, AGNs, solar flare, and so on [1]. TeV gamma rays, however, have been detected only from three-types of those objects: pulsar/nebulae, SNRs, and AGN. All TeV gamma-ray sources

are summarized in the Table I with the classification of the sources by Weekes [8]. There are only four sources established by multiple observations, and several possible candidates are now waiting the reconfirmation. In particular AGN, pulsar/nebula and shell-type SNR are very promising sources. Since lots of articles already have described the high energy phenomena in AGN [24), 25)], here we concentrate on discussion of the galactic TeV gamma-ray sources, SNRs and pulsar/nebulae, of which the majority have been found and studied by the CANGAROO group.

3.1. Pulsar/nebulae

The Crab is a famous celestial high energy object, comprising the youngest pulsar born in 1054 with a fast rotation period of 33 ms and a surrounding synchrotron nebula activated by the intense relativistic wind from the pulsar. The Crab emits both pulsed and unpulsed gamma rays in the GeV region. The pulsed component is emitted from the interior of the light cylinder of the pulsar, due to the curvature radiation of the high energy electrons driven by electromagnetic force which is generated by the rotation of the strongly magnetized pulsar ($\sim 10^{12}$gauss).

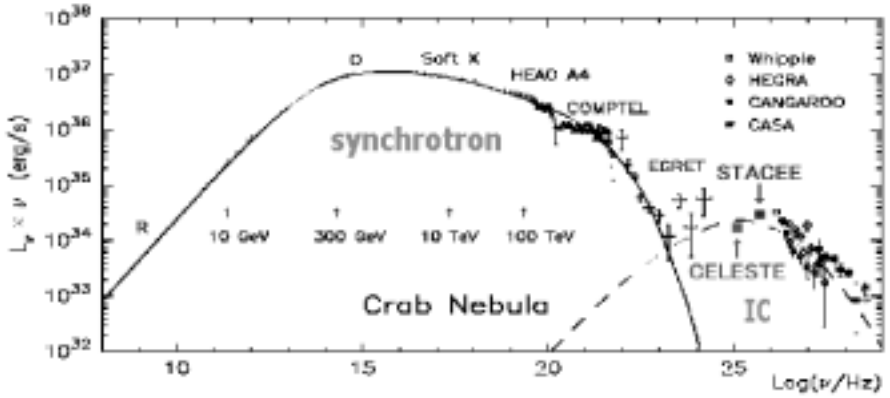

Fig. 6. Overall spectrum of unpulsed emission from the Crab, and SSC model is fitted.

The pulsed spectrum observed by EGRET strongly suggests its termination between 10 GeV$\sim$ 100GeV [26)], which is well consistent with theoretical predictions [27), 28)]. On the other hand, above 100 GeV only unpulsed spectra have been observed by lots of IACTs. Unpulsed gamma rays are considered to be generated by the strong shock caused by the collision with the intense relativistic wind and the environmental ISM around the pulsar, which probably accelerates electrons up to 10^{15}eV around the shock front. Those high energy electrons emit unpulsed very high energy gamma rays over 10^{14}eV through IC scattering with synchrotron photons(radio to MeV gamma-ray regions) emitted by themselves in the magnetic field of the nebula($\sim 300\mu$ gauss) [29) - 31)]. This magnetic field yields huge number of synchrotron photons, and its energy density exceeds that of CMB. This generation process is widely known as Self-Synchrotron Compton model (SSC) [32)], and is also considered as a main process of TeV gamma-ray emission from blazars [32)]. Blazars are AGNs emitting strong synchrotron light violently, and a plenty of them also emit high energy gamma rays.

All AGN emitting TeV gamma rays belong to blazars. Figure 6 shows the overall spectrum of the unpulsed emission from the Crab fitted by the SSC model. The SSC model well fit the wide range of the spectrum with reasonable magnetic field strength. Actually clear X-ray images obtained by Chandra undoubtedly shows the synchrotron torus surrounding the pulsar generated by the termination shock of the pulsar wind [33]. Thus the high energy phenomena around the Crab pulsar and nebula have been understood quite well.

In addition, since the emissions of both pulsed and unpulsed gamma rays from the Crab are constant and intense, it is often observed as a standard candle source. As shown in Fig.6, several data are plotted and considerably consistent. Note that the CANGAROO group alone observed it from the southern hemisphere and provided the highest energy spectrum above 20 TeV by large zenith angle observation [34].

The only unobserved region in its spectrum is $10 \sim 100$ GeV, but the GLAST, next gamma ray satellite to be launched in 2005 [35], and larger IACTs will soon uncover this area.

PSR1706-44 is the second persistent object in the TeV region classified in rank A, which was detected by CANGAROO in 1995 [5]. It is a relatively young pulsar with the period of 102ms, of which rotational energy loss is the fourth of existing thousand pulsars.

It emits only pulsed gamma rays in the GeV region [36], but unpulsed ones were observed in both TeV [37] and X-ray regions [38]. Though a faint nebula around the pulsar was reported by radio [39] and X-ray observation [40),41], respectively, those two features looks unlike. Anyway this pulsar has no intense synchrotron nebula such as the Crab.

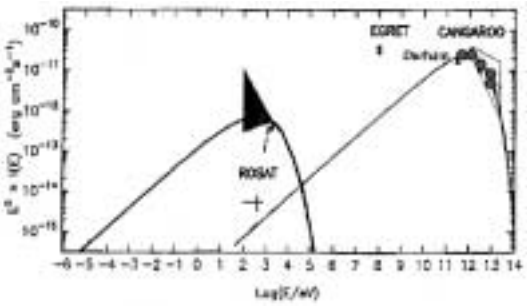

Fig. 7. Overall energy spectrum of unpulsed emission of PSR1706-44.

Figure 7 shows its overall energy spectrum of the unpulsed emission, where observational results in X-ray [40),41] and TeV gamma rays [5),42], and the theoretical prediction [43] are presented. In addition, the preliminary result obtained in 1999 by the new 7m Čerenkov Telescope of CANGAROO is plotted in 0.6 – 4 TeV. Since the synchrotron nebula, even if it exists, is very faint, the magnetic field strength seems to be the same order of that in the galactic space, and hence the energy density of CMB far exceeds that of synchrotron radiation in the nebula. In such a circumstance, high energy gamma rays are expected to emanate thorough IC scattering of high energy electrons with the CMB. Because the energy density of CMB is constant in all space and well-known, the energy spectrum of IC radiation of PSR1706 can be predicted fairly quantitatively using its synchrotron spectrum, similar to the case of SN1006, as shown in Fig.7. It is noticed that the peak energy flux of synchrotron radiation is quite less than that of IC radiation, and hence the estimated magnetic field is considerably weak ($\sim$ 1 μgauss). Taking account of both the faint nebula and the very weak

magnetic field, the high energy phenomenon around PSR1706 seems to be dissimilar to the Crab nebula. For example, Aharonian, Atoyan and Kifune considered that synchrotron X-rays and IC TeV gamma rays are generated in different positions in the nebula; X rays are generated in the inner region of which magnetic field is relatively strong and TeV gamma rays are in the outer region. Their predicted spectrum are drawn in Fig. 7 [43].

Recently we have obtained the two TeV gamma-ray spectra of PSR1706; one is between 1.5 and 10 TeV from 1997 data observed by the 3.8m CANGAROO telescope [44], and the other is between 0.6 and 5 TeV from 1999 data observed by the new 7m CANGAROO II telescope respectively. Those are plotted in Fig. 8, where obtained differential fluxes are converted to integral ones for the comparison with other data. One can see a break in the power law around 1 TeV where the power index varies from -3.0 to -1.8. This significant steepening of the spectrum is consistent with the prediction of IC process in the scattering of CMB. Now the analysis of new data obtained by the 10m CANGAROO III telescope is under way, of which result will cover wider energy range from $\sim$0.2TeV with higher statistics.

Unpulsed TeV gamma-ray emission from the Vela pulsar was also detected by CANGAROO in 1997 [45]. Vela is a famous pulsar which is the brightest celestial object in the GeV region, and surrounded by a huge Vela SNR. Its synchrotron nebula was observed in X-rays by several satellites [46),47]. It is worth noting about Vela is that the detected TeV gamma-ray emission point is about $0^\circ.13$ apart from the pulsar position. The detail is described in the reference [45]. Now we are observing the Vela in 2001 to reconfirm the emission of TeV gamma rays.

Recently Chandra has provided the very clear X-ray images and made clear the structures of the Crab nebula [33] and the Vela nebula [48]. Chandara also has observed PSR1706 and some other pulsars, and soon their image will be revealed. Using those new data such as clear X-ray images and wide TeV spectra, the understanding of high energy phenomena around a pulsar would advanced drastically.

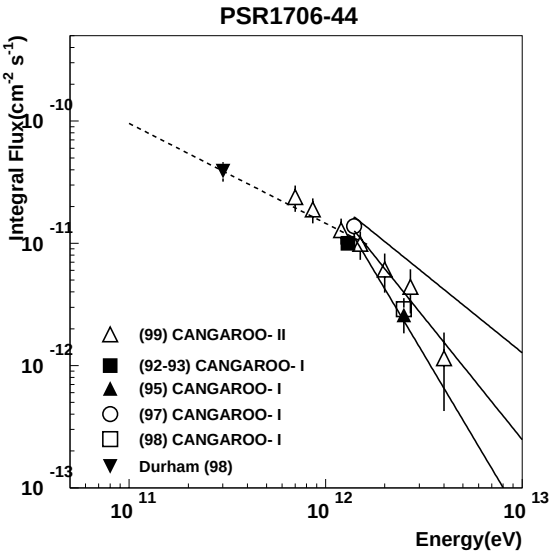

Fig. 8. Preliminary Spectrum of PSR1706 between 0.6 TeV and 5 TeV observed by 3.8m CANGAROO telescope and 7m telescope, where differential fluxes are converted to the integral ones for the comparison with other data.

3.2. Shell-type Supernova Remnants

In the second section, particle acceleration in SNRs, in particular TeV gamma-ray emission of SN1006 (shell-type SNR), is described. Here other two intriguing TeV sources of shell-type SNR are discussed. RXJ1713.7-3946 was observed as the strongest synchrotron X-ray emitter among SNRs by ASCA in 1997 [49], and subsequently TeV emission was detected from the maximum emission point of X-ray as shown in Figs.9 [15]. We have observed this point again in 1999 using the 7m telescope, and detected the enhancement of the alpha plot as shown in Fig. 10 (preliminary data), which indicates the detection of gamma rays from the source as described in section 4.1.

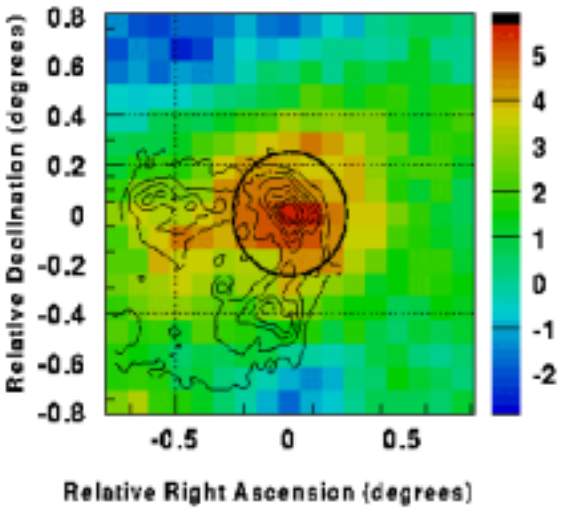

Fig. 9. Map of TeV gamma-ray emission of RXJ1713 observed by 3.8m telescope with the contours of X-ray emission by ASCA

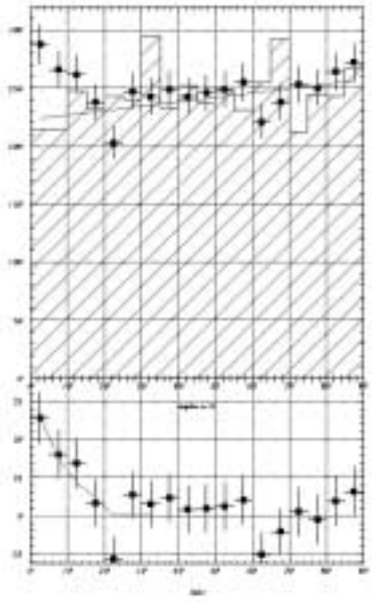

Fig. 10. Preliminary Alpha plots of RXJ1713 for both on source (dotted) and off (hatched) obtained from the 1999 data using the 7m CANGAROO telescope.

Assuming IC process generates TeV gamma rays, the magnetic field strength is estimated from both X-ray and TeV gamma-ray flux to be $\sim 11\mu$ gauss. Its morphology is more complex than that of SN1006, of which north parts might interact with the molecular cloud observed by the radio telescope [50]. Therefore this TeV emission might be ascribed to π° decay generated by the collision of accelerated protons in this SNR with the molecular cloud. The image of TeV gamma rays in Fig. 9 clearly indicates the extension of the emission region over the point-spread function of the telescope. This extension toward the dense region of the molecular cloud might support the existence of π° decay emission. Soon we will give detailed data for this question from the stereo observation using the next 10m telescopes (CANGAROO-III): the wide spectrum from 0.3 to 10 TeV and the real image of

TeV gamma-ray emission with the angular resolution of 0.1°. Cassiopeia A in the northern hemisphere is the youngest SNR, and recently the HEGRA group has reported a detection of TeV gamma-ray emission of $\sim 3 \times 10^{-13} cm^{-2} s^{-1}$ with 5σ statistical significance from this SNR [16]. Cas-A is a quite different type SNR from SN1006 and RXJ1713; it is very dense and emits strong thermal X-rays peaking around a few keV. However, non-thermal hard X-ray emission above 50 keV has been detected in 1998 [51]. The HEGRA group suggests that these TeV gamma rays are due to the π° decay by modeling the overall spectrum of Cas-A.

Observations with full imaging and wide band spectroscopy definitely make it possible the quantitative study of diffusive shock acceleration occurred inside SNRs. In particular the angular resolution of 0.1 degree to be achieved by the stereo observation of Čerenkov telescopes is enough for the morphological study of SN1006 and RXJ1713. These requirements will be soon realized by the next generation of IACTs. In near future, we would make clear how particles are accelerated in SNRs using the CANGAROO III telescopes mentioned hereafter.

§4. Observation of Celestial TeV Gamma Rays

4.1. Imaging Air Čerenkov Technique

High energy cosmic rays coming to the atmosphere interact with molecules of the air. Primary particles are classified as electromagnetic particles (electrons, positions, and gamma rays) and hadrons (mainly protons). In the air, successive interactions increase the number of secondaries (electrons, gamma-rays or hadrons) exponentially, This phenomenon is well known as an Extensive Air Shower (EAS). However the development of EAS eventually ceases in the atmosphere by consuming their energies. EASs caused by electromagnetic primaries develop through electromagnetic processes in the atmosphere.

On the other hand cosmic-ray nuclei generate nuclear cascades comprising both electromagnetic and hadronic secondaries (mainly pions). Secondary π°s decay into two gamma rays, and originate electromagnetic cascades thereafter. Energetic $\pi^\pm$s greater than 10 GeV further interact with atmospheric nuclei, and generate more pions. Finally less energetic $\pi^\pm$s decay to muons in the atmosphere which come to the ground without decaying. The simulated developments of EAS initiated by a proton and a gamma ray are depicted 3-dimensionally in Fig. 11. As shown in this figure, a hadronic shower become transversely more extended than a gamma-ray shower due to their larger transverse momenta of secondaries.

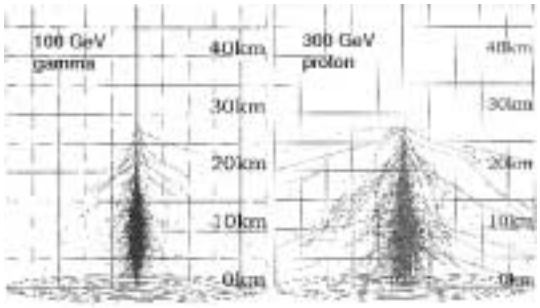

Fig. 11. Simulations of developments of EAS initiated by gamma rays(100GeV) and protons(300GeV).

Figure 12 shows the schematic image describing the principle of the imaging air Čerenkov technique. In EASs, Čerenkov photons are radiated by relativistic charged secondary particles of which velocity exceed light velocity in the atmosphere. Even for a relatively low-energy shower of which secondary particles terminates in the middle of the atmosphere, a large fraction of emitted Čerenkov photons can reach on the ground. The total number of Čerenkov photons radiated from an EAS is proportional to the integrated path length of almost all electrons and positrons in the EAS, and then the shower energy can be known from the amount of Čerenkov light. The maximum of the shower development is generally located around the altitude of ∼10,000m with little dependence on its energy, and also the emission angles of Čerenkov lights are collimated within one degree. Therefore the area in which Čerenkov photons are spread is estimated to be $\sim 10^4\ m^2$ from above two parameters. It is much larger than the typical detection area of a satellite of $\sim 1m^2$. Moreover, because of the independence of the area on the shower energy, the density of Čerenkov photon detected by a telescope on the ground become a good estimator for the energy of a primary particle. For example an EAS initiated by an 1 TeV primary gamma ray produces the only $20 \sim 50\ photons \cdot m^{-2}$ in $350 \sim 550\ nm$ at the sea level. The large reflectors collecting many Čerenkov photons are therefore inevitable for the efficient detection of VHE gamma-rays. Although a modern large 10m diametrical mirror collects about ∼ 2000 photons from an 1 TeV gamma ray, the number of photons detected by photomultipliers decreases to about ∼ 400 photons by the low quantum efficiency of PMT (∼ 20%). On the other hand, the timing duration of Čerenkov photons concentrates within less than 20ns on the ground, which enables to discriminate Čerenkov photons from huge number of night sky background photons. For a 10m class mirror, gamma rays of less than 100 GeV can be detected.

A gamma-ray flux even from a strongest source such as the Crab nebula is only $\sim 10^{-11} cm^{-2} sec^{-1}$ above 1 TeV, while the cosmic-ray background flux is $\sim 10^{-5} cm^{-2} sec^{-1} str^{-1}$ above 1 TeV. Assuming the field of view of a telescope of 10^{-3} str ($\sim 1^\circ$ radius), the signal-to-noise ratio is estimated from above fluxes to be $\sim 10^{-3}$, which had made very difficult to detect celestial TeV gamma rays for a long time.

The imaging technique provides us both good angular resolution of $\sim 0^\circ.1$ ($\sim 1^\circ$ for non-imaging telescopes) and efficient suppression of hadron showers, which improves the signal-to-noise ratio by about 100 times. This procedure is schematically drawn on the focal plane image of Fig.13. Čerenkov light collected by a reflector make an image on the focal plane, which is a projection of the shower development onto the focal plane, and is elongated along the shower axis. Consequently Čerenkov images of gamma-ray showers ("gamma-ray images") elongate to the source position in the filed of view, and hence directs toward the center of the camera pointing to the source. On the other hand, images generated by cosmic-ray nuclei ("hadronic images") have random directions in the field of view due to the random injection of primary cosmic nuclei and the irregularity of the shower development. In the imaging technique, Čerenkov images are detected by an camera comprising fine pixel-photon detectors for which PMTs are usually used.

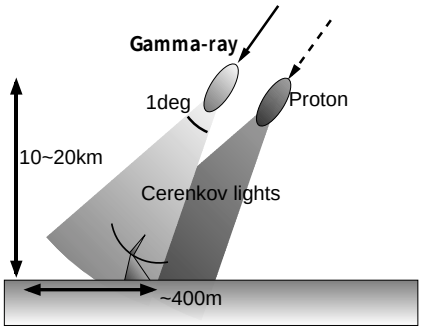

Fig. 12. Schematic image describing the principle of air Čerenkov technique.

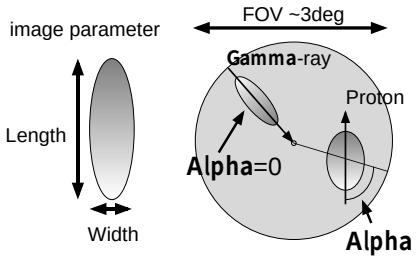

Fig. 13. Schematic view describing the parameterization in imaging air Čerenkov technique.

In 1985, Hillas proposed the parameterization of the Čerenkov image by means of fitting an ellipse to it, and showed that these fitting parameters can be used to enhance gamma-ray signals [6]. In 1989, the Whipple group and soon later the CANGAROO group detected high energy gamma-ray signals using this technique and proved the validity of this technique. Within a few years this technique became common technique to detect celestial TeV gamma rays. Image parameters are described in Fig. 13. Hadronic images are generally broader in Width, longer in Length due to the irregular and wide-spread developments of their showers than those in gamma-ray showers. Orientation angle, called Alpha, of hadronic showers should be distributed uniformly between 0° and 90°, while alpha of gamma-ray showers concentrates around 0°.

4.2. Stereo Observation

A Čerenkov image observed by single IACT provides only the information about the plane defined by the shower axis and the position of the telescope. The direction of the shower, namely the direction of the source, can be determined as a cross line of above two planes of two images observed for the same shower from different positions, as shown schematically in Fig14. Figure15 depicts the overlaid images in the field of views of the two telescopes observed from different angles as shown in Fig14. The true direction of the shower corresponds to θ in this figure, which can be determined for every shower. Thus the real image of celestial gamma-ray distributions in the sky can not be obtained without simultaneous observations for the same source by multiple IACTs.

A morphological study is particularly important for extended sources like SNRs or galaxies. Also the rejection power of a hadron shower is drastically improved by more 10 times using the several images for one shower. The HEGRA group was the first who revealed these capabilities of stereo observation using the five 3m IACTs in 1997 [55]. The detailed study of the stereo technique with multiple 10m class IACTs was also carried out by them [52), 53]. Figures 16 and 17 shows the simulated performances of the effective area and angular resolution of the stereo observation by several 10m IACTs, which were estimated for the design of the CANGAROO-III telescopes. These results are consistent with other studies for the next generation

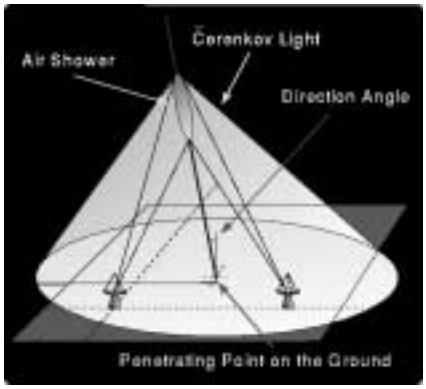

Fig. 14. Schematic diagram describing the principle of stereo observation.

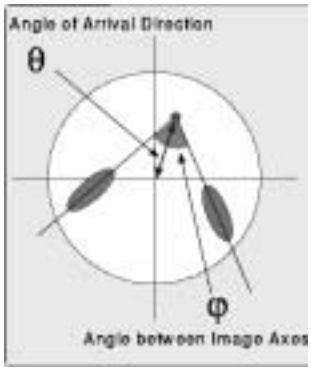

Fig. 15. Overlaid images in the field of views of the two telescopes observed from different angles in stereo observation. True direction of the shower corresponds to θ.

IACTs. Nowadays the stereo observation is generally expected to give us both the real imaging with angular resolution of less than 0.1 degree and the good sensitivity of $\sim 10^{-13} cm^{-2} s^{-1}$.

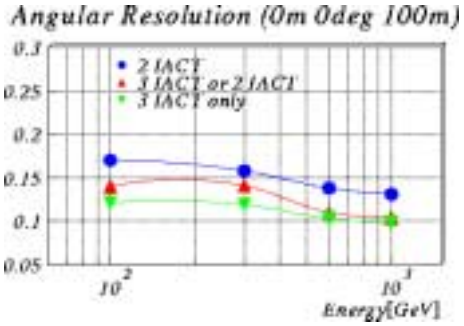

Fig. 16. Simulated performances of the angular resolution of the stereo observation using several 10m IACTs designed for CANGAROO-III.

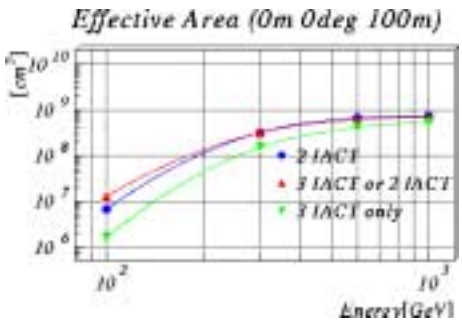

Fig. 17. Simulated performances of the effective area of the stereo observation using several 10m IACTs designed for CANGAROO-III.

§5. Imaging Air Čerenkov Telescopes in the World

As mentioned above, Imaging Air Čerenkov technique has been recognized as the main stream of very high energy astronomy. Current experiments using the imaging technique are summarized in Table II. The Whipple group succeeded in eliminating more than 99 % of the background events by using the imaging technique in their analysis [54]. They have found three VHE gamma-ray sources in Class A as listed in Table I Also in the southern hemisphere the CANGAROO group has found four TeV gamma-ray sources in Class A and B using the finest pixel imaging telescope at that time. The HEGRA group is a pioneer of stereo observation using multiple IACTs [55]. An array of five 3m telescopes is operated in the Canary Islands, and they

have recently detected TeV gamma rays from Cas-A. The detection of Cas-A, the weakest source in TeV sources, has dramatically demonstrated the strong rejection power for hadron showers by stereo observation.

Experiment	Mirrors	A(m^2)	PMTs	FOV(deg)	σ_θ(deg)	R_{CR} (Hz)	E_{th} (TeV)
CANGAROO	2	11	256	3.0	0.18	1	1.5
CAT	1	18	600	4.8	0.1	15	0.25
Durham Mark 6	3	42	109	3.4	0.1	17	0.25
GT-48	2	27	37	2.7	0.2	2	0.90
HEGRA-CT	6	9	271	4.6	0.1	15	0.50
Nooitgedacht	4	7	4	1.7	1.7	3	0.70
Pachmari	25	4	1	3.0			
SHALON	1	10	144	7.2	0.4	5	1.0
TACTIC	4	10	349	2.8			
Telescope Array	3	6	256	4.5	0.1	6	0.50
Whipple	1	75	151	3.5	0.1	18	0.25

Table II. Characteristics of major atmospheric Čerenkov telescope in 1997. The number of distinct mirrors is given,followed by some characteristics: mirror area (A), the number of PMTs in the camera, the field of view (FOV), the angular resolution (σ_θ), the cosmic-ray rate (R_{CR}), and the energy threshold (E_{th}).

After the active decade of 1990's, above three groups are now extensively promoting next generation IACTs aiming for full imaging by stereo observation and wide band spectroscopy from sub to multi TeV. The design concepts of the telescopes proposed by those groups are quite similar except MAGIC (one part of HEGRA). As a next generation of IACTs, an array of several 10m-class large telescopes having a fine pixel imaging camera with 500 $\sim$ 800 photomultipliers covering the large FoV of $\sim 4^\circ$ are common in VERITAS(extension of Whipple) [56], CANGAROO-III [57], and HESS(the other part of HEGRA) groups [58]. Expected features for energy threshold, sensitivity, and angular resolution are $\sim$ 100 GeV, $1 \sim 5 \times 10^{-13} cm^{-2} s^{-1}$, and ≤ 0.1 degree, respectively. The MAGIC group is constructing a huge single 17m telescope to aim for very low energy threshold of $\sim$ 50GeV in the Canary islands [59].

Until 2001 those four projects have been approved. the CANGAROO group has completed the first 10m telescope in 2000, and will construct the four telescopes until 2004 as mentioned below. The HESS group is constructing the first 12m telescope with a large camera consisting of $\sim$ 800 photomultipliers, and three of same-type telescopes will be completed in 2002 or 2003 in Namibia. The VERITAS group has just begun the construction of the first 10m telescope near the Whipple observatory in New Mexico, USA. They will construct a hexagonal array of 7 telescopes in several years.

In 2005, those four groups will start the full operation of the new telescope systems.

5.1. CANGAROO-III Project

As an example of the next generation of Air Čerenkov Telescopes, i.e., an array of 10m class IACTs for stereo observation in the sub-TeV region, CANGAROO-III is briefly introduced.

The CANGAROO-III is a project to study celestial gamma rays in the sub TeV region utilizing a stereoscopic observation of Čerenkov light with an array of four 10m IACTs[57], following the CANGAROO-I 3.8 m telescope[7] and the CANGAROO-II 7 m telescope constructed in March 1999 [60) 61) 62)] in Woomera, South Australia (136°47′E, 31°06′S, 160m a.s.l.). It has officially started since April 1999 and is planned as a five-year program. In February 2000 the 7 m telescope has been expanded to a 10 m telescope by doubling the number of small mirrors as shown in Fig. 18, which is the first telescope of the CANGAROO-III array. Subsequently we are making the second telescope system in Japan, which will be shipped and installed in 2001. Other two telescopes will be installed successively in the fourth and fifth years.

	10m telescope
Focal length	8m Prabola
80cm CFRP mirrors	114 (53m²)
Number of PMTs	552 (1/2") FOV ~ 3° (4°)
Electronics	TDC & ADC
Point image size	0.20° (FWHM) (< 0.15°)

Fig. 18. The 10 m telescope completed in February 2000 in Woomera, South Australia.

Each telescope will be set on a corner of a diamond of about 100 m side as shown in Fig.19. The first stereoscopic observation will be performed in 2002 and the full four telescopes will be in operation in 2004. The most mark point of this telescope is the first use of plastic mirrors for an IACT so far. The detail of this plastic mirror and the total structure of the 7 m telescope is described elsewhere [63)]. Although the ability of focusing is a little worse than that of a glass mirror, it has many advantages such as light weight, hardness, and durability. The image of a star was measured with a CCD camera and its size (FWHM) is 0.20°. This is a little larger than the pixel size and also the design value which is a little smaller than the pixel. Now the refinement of the focusing of plastic mirrors is intensively underway, and we expect the image size of the 2nd telescope will be improved about two thirds of that of the first telescope. This improvement will reduce the energy threshold for gamma rays from ∼300 GeV to ∼150 GeV.

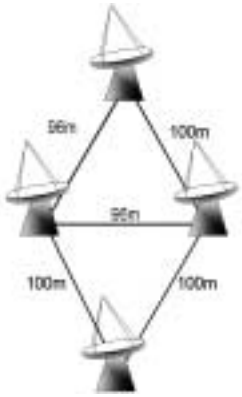

Fig. 19. Arrangement of the array of CANGAROO-III four telescopes.

The camera consists of 552 PMTs of half-inch diameter and subtends about 3 degrees in octagon shape. On each PMT a light guide made of plastic coated by aluminum is attached to collect photons focused on the focal plane more efficiently. The inner part within 2 degrees are used for the trigger decision to optimize the figure of merit of the detection efficiency of gamma-ray showers. Signals from the PMTs are fed into analog-buffer amplifiers. One output goes to the existing front-end module (discriminator and scaler) and the other goes to newly developed VME-based ADCs

(12 bit resolution, 0.25 pC/count, 150 ns internal delay, 50 ns gate width). The discriminated signals are sent to TDCs to measure timing with 1ns resolution, which enable us to reject almost all the accidental photons due to the night sky background despite of the wide ADC gate; actually ∼20 ns gate is achieved at the offline analysis.

Observation and Result

Observations using both the 7m and the 10 m reflector in 1999 and 2000 are summarized in Table III. Target objects were primarily selected from our list of TeV gamma-ray sources: SN1006, PSR1706-44 and RXJ1713.7-3946 in order to reconfirm our previous detections with the 3.8m telescope, and furthermore to obtain energy spectra of those galactic sources from sub to multi TeV. Also nearby X-ray selected BL Lacs (some type of blazars): PKS2005-489, PKS2155-304 were observed along with multi wavelength campaigns.

1999	2000
PSR1706-44	SN1006
RXJ1713.7-3946	PSR1706-44
PKS2005-489	RXJ1713.7-3946
PKS2155-304	PKS2005-489
PKS0548-322	PKS2155-304
Crab	PSR1259-63
	NGC253

Table III. Celestial objects observed by CANGAROO telescope in 1999 and 2000

Preliminary results of the Crab in 1999 are shown in Figs.20 and 21. The spectrum of the Crab obtained from the alpha peak is well consistent with the previous data of the CANGAROO-I and also other data above 4 TeV. The differential flux of PSR1706 is already presented and discussed in the previous section. Those preliminary data compared with a Monte Carlo simulation suggests the threshold energy of the 7m telescope is 600∼700 GeV depending on their power indices. Another significant result obtained by the 7m telescope is the reconfirmation of the TeV emission of RXJ1713 which is the second candidate of SNR emitting TeV gamma rays, as shown shown in Fig.10. The analysis for the data obtained by 10m telescope is underway, and larger peak in the α plot has been probably observed. The coarse estimation of the integral flux of $\sim 10^{-10} cm^{-2} s^{-1}$ at ∼500GeV suggests that RXJ1713 may be the most intense TeV gamma ray source in the southern hemisphere. The result will soon appear.

Work in progress for New telescopes

As mentioned above, the refinement of the plastic mirror is most significant. In addition, some important improvements are being carried out as follows. The new design of a camera will be in hexagonal shape so that the dead space between PMTs is minimal. The field-of-view will be enlarged to 4.3° with 427 3/4" PMTs (Hamamatsu R3478) to optimize the efficiency of stereo observation. The new electronics system will be all VME-based. The front-end circuit (under development, 16 ch/VME-9U) amplifies the signal and feeds to an ADC (the improved type of those used in the CANGAROO-II with faster conversion), discriminates it and feeds to a TDC, an internal scaler and a trigger circuit.

In order to decrease the energy threshold, huge number of accidental coincidence of hit PMTs in the camera has to be excluded at the trigger level. The pattern trigger is considered as a fairly effective method, and recently has been adopted for several

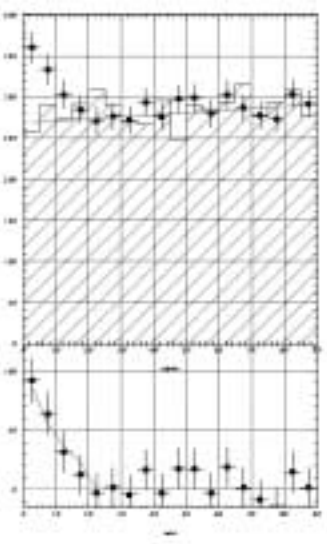

Fig. 20. Preliminary alpha plots of the Crab for both on source (dotted) and off (hatched) observed by 7m CANGAROO-II telescope in 1999.

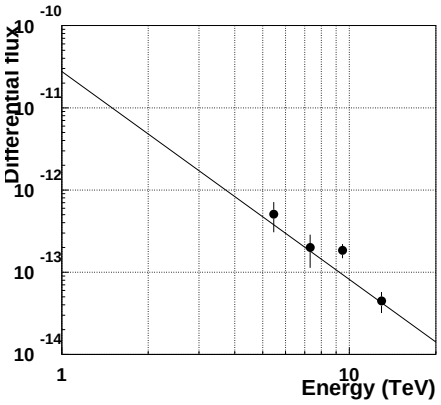

Fig. 21. Preliminary differential flux of the Crab of 1999 observations observed by 7m CANGAROO-II telescope with the average flux obtained from the world data.

IACTs. The pattern trigger circuit using Programmable Logic Device are under development, which will be expected to decide the trigger within 100ns. Increased data size requires faster data acquisition. Now we are testing several possibilities including VME-based Pentium CPU board running a Linux operating system, which shows faster task switching, reducing dead time of data acquisition.

Those developments will be adopted for the second telescope constructed in 2001. Final goal of the ability of the CANGAROO-III four 10m telescope array(Fig.22) is followings: the energy threshold of ~ 100 GeV, the sensitivity of $\sim 5 \times 10^{-13} cm^{-2} s^{-1}$ at 500 GeV, and the angular resolution of ≤ 0.1 degree.

§6. Summary

GeV and TeV gamma-ray astronomy has been established in 1990's due to the successful discoveries of many unexpected celestial objects emitting gamma rays. Last year Compton Observatory has been quit and disappeared, however the next advanced satellite of high energy gamma-ray observation, GLAST, would not be available until 2005. On the other hand the next generation IACTs, the arrays of several 10m IACTs (CANGAROO,HESS,VERITAS), and the huge 17m mono IACT (MAGIC) will soon appear until 2002 and exploit the sub TeV region. In particular, they are expected to make clear the cosmic-ray origin in the galaxy as mentioned above. After the launch of GLAST in 2005, almost all the energy region from 100 MeV to 100 TeV will be covered without energy gap by the satellite and IACTs, and hence several thousands celestial gamma-ray sources would be found such as the

Fig. 22. An imaginary picture of the CANGAROO-III array appearing in 2004.

present X-ray astronomy.

Acknowledgments

I would like to thank Nishinomiya city and Prof. F.Takahara for giving a chance to talk at famous Yukawa memorial International Symposium. Also the cooperation and encourage of colleagues of the CANGAROO group are very appreciated.

References

1) R.C. Hartmann, et al., Astrophys. J. Suppl. **123** (1999), 79
2) G. Vacanti,et al., Astrophys. J. **377** (1991), 467
3) M. Punch,et al., Nature **358** (1992), 477
4) J. Quinn ,et al., Astrophys. J. **456** (1996), L83
5) T. Kifune ,et al., Astrophys. J. **438** (1995), L91
6) A.M, Hillas, Proc. 19th Int. Cosmic-Ray Con.(La Jolla), 3, 1985, 445.
7) T. Hara,et al., Nucl. Instrum. Methods Phys. Rev. **A332** (1993), 300
8) T.C. Weekes, Proc. of GeV - TeV Gamma Ray Astrophysics Workshop(Snowbird),eds B. Dingus et al., 3
9) M. Pohl, Astron. Astrpophys. **307** (1996), L57
10) A. Mastichiadis, Astron. Astrpophys. **305** (1996), L53
11) A. Mastichiadis and O.C. Jager, Astron. Astrpophys. **311** (1996), L5
12) T. Yoshida and S. Yanagita, in Proc. 2nd INTEGRAL Workshop 'Transparent Universe, ESA SP-382,(1997), 85.
13) T. Tanimori ,et al., Astrophys. J. **497** (1998), L25
14) R. Willingale et al., Mon. Not. R. Astron. Soc. **278** (1996), 749
15) H. Muraishi ,et al., Astron. Astrpophys. **354** (2000), L57
16) G. Pühlhofer, et al. Proc. of the 26th ICRC (Salt Lake City), **3**, 1999, 492.
17) M. Teshima see his article in this proc. 2001
18) L.O'C. Drury, W.J. Markiewicz and W.J. Volk, Astron. Astrpophys. **225** (1989), 179
19) R.D. Blandford and D. Eichler, Phys. Rep. **154** (1987), 1
20) R. , Phys. Rep. **154** (1987), 1
21) L.I. Sedov, LaTeX: Similarity and Dimensonal Methods in Mechanics (Academic Press, 1959).
22) K. Koyama,et al., Nature **376** (1995), 255
23) T. Naito,et al., Aston. Nachr. **320** (1999), 205

24) R. Ong, Phys. Rep. **305** (1998), 93
25) M. Catanese and T.C. Weekes, Publ. Astron. Soc. of Pacific **111** (1999), 1193
26) M.P. Ulmer, et al., Astrophys. J. **432** (1994), 228
27) J.K. Daugherty and A.K. Harding, Astrophys. J. **458** (1996), 278
28) R.W.Romani, Astrophys. J. **470** (1996), 469
29) O.C. De Jager and A.K. Harding, Astrophys. J. **396** (1992), 161
30) A.M. Atoyan and A.F. Aharonian, Mon. Not. R. Astron. Soc. **278** (1996), 525
31) A.M. Hillas et al., Astrophys. J. **503** (1998), 744
32) R.J. Gould, Phys. Rev. Lett. **15** (1965), 511.
33) C. Martin et al., Astrophys. J. **536** (2000), L81
34) T. Tanimori et al., Astrophys. J. **492** (1998), L33
35) P.F. Michelson, et al. GLAST, Large Area Telescope Flight Investigation, (http://www-glast.stanford.edu/pubfiles/proposals/bigprop/), (1999).
36) D.J. Thompson et al., Astrophys. J. **465** (1996), 385
37) D.I. Nel et al., Astrophys. J. **418** (1993), 836
38) H.A.K. Ray and M.S. Stickman, Proc. of 4th Compton Symp.(New York), AIP, Universal Academy Press, (1997), 607.
39) O.J. McAdam and M. Parkinson, Nature **361** (1993), 516
40) K.B.W. Becker et al., Astron. Astrpophys. **298** (1995), 528
41) Y.S. John et al., Astrophys. J. **493** (1998), 884
42) P.M. Chadwick et al., Astropart. Phys. **9** (1998), 131
43) F.A. Aharonian, A.M. Atoyan and T. Kifune, Mon. Not. R. Astron. Soc. **291** (1997), 162
44) M. Moriya, Ph.D. Thesis, Study of Very High Energy Gamma Ray from the Pulsar Nebula around PSR1706-44, Tokyo Inst. of Tech., 1999.
45) T. Yoshikoshi et al., Astrophys. J. **487** (1997), L95
46) C.B. Markwardt and H. Ogelman, Nature **375** (1995), 40
47) C.B. Markwardt and H. Ogelman, Astrophys. J. **480** (1997), L91
48) http://chandra.harvard.edu
49) K. Koyama et al, Publ. Astron. Soc. Japan **49** (1997), L7
50) P. Slane et al., Astrophys. J. **525** (1999), 357
51) G.E. Allen et al., Astrophys. J. **487** (1997), L97
52) F.A. Aharonian et al., Astropart. Phys. **6** (1997), 343
53) F.A. Aharonian et al., Astropart. Phys. **6** (1997), 369
54) P.T. Reynolds et al., Astrophys. J. **404** (1993), 206
55) A. Daum, A. et al.,Astropart. Phys. **8** (1997), 1
56) T.C. Weekes et al., VERITAS proposal (http://earth.purdue.physics.edu/veritas), 1999.
57) M. Mori et al., GeV-TeV Gamma Ray Astrophysics Workshop (eds. B.L. Dingus et al.), AIP Proceedings **515**,(2000),485.
58) W. Hofmann et al.,GeV-TeV Gamma Ray Astrophysics Workshop (eds. B.L. Dingus et al.), AIP Proceedings **515**,(2000),500.
59) J.A. Barrio, et al. MPI-Ph/E98-5, (1998).
60) T. Tanimori et al., Proc. 26th ICRC (Salt Lake City, Utah, USA), OG.4.3.04 (1999).
61) M. Mori et al., Proc. 26th ICRC (Salt Lake City, Utah, USA), OG.4.3.31 (1999).
62) H. Kubo et al., GeV-TeV Gamma Ray Astrophysics Workshop (eds. B.L. Dingus et al.), AIP Proceedings **515**, (2000), 313.
63) A.Kawachi et al., Astropart. Phys. **14** (2001), 261